On the theory and computation of anisotropic damage at large strains

Andreas Menzel – Paul Steinmann

Chair of Applied Mechanics, Department of Mechanical Engineering,
University of Kaiserslautern, P.O. Box 3049, D-67653 Kaiserslautern, Germany
amenzel@rhrk.uni-kl.de, ps@rhrk.uni-kl.de,
mechanik.mv.uni-kl.de

ABSTRACT. *The goal of this contribution is the formulation and algorithmic treatment of anisotropic continuum damage mechanics at large strains. Based on the concept of an isotropic, fictitious and undamaged configuration a Finger–type damage metric tensor in terms of the fictitious linear tangent map is introduced. Referring to the principle of strain energy equivalence with respect to the fictitious, effective space and the standard reference configuration the free Helmholtz energy can be formulated within the standard reference configuration and treated in the spirit of standard dissipative materials. Thereby, the introduced damage potential substantially affects the anisotropic nature of the damage formulation. Finally, some numerical examples demonstrate the applicability of the proposed framework.*

RÉSUMÉ. *L'objectif de cette contribution est la formulation théorique ainsi que les aspects algorithmiques d'un modèle d'endommagement anisotrope en transformations finies. Un tenseur métrique (tenseur de Finger) d'endommagement est introduit en terme d'application linéaire tangente fictive basée sur le concept de configuration fictive, anisotrope et non endommagée. En utilisant le principe de l'équivalence en énergie dans l'espace fictif des variables effectives et la configuration de référence, l'énergie libre de Helmholtz est formulée comme potentiel d'état dans le cadre des milieux dissipatifs standards généralisés. Le potentiel d'endommagement introduit est substantiellement sensible à la nature anisotrope de l'évolution de l'endommagement. Enfin, des examples numériques sont traités pour illustrer les performances du modèle proposé.*

KEY WORDS: *damage mechanics, anisotropy, finite deformations*

MOTS-CLÉS: *endommagement, anisotropie, transformations finies*

MSC (2000): *74R05, 74E10, 74A20, 74S05*

1. Introduction

The main objective of this work is the development of a phenomenological, geometrically nonlinear formulation of anisotropic tensorial second order continuum damage.

In fact, it is the evolution of microscopic internal structure of materials by nucleation and growth of distributed microcracks or microvoids which in turn leads to the deterioration of the mechanical properties of the material. Especially the shape, orientation and evolution of these microdefects show a significant dependence on the direction of stress and strain. Obviously, the nature of damage is anisotropic and thus a continuum damage theory should provide sufficient freedom to capture these anisotropic damage effects.

The appropriate choice of the physical nature of mechanical variables describing the damage state of a material and their tensorial representation is since long under discussion, for an overview see e.g. Lemaitre [LEM 96] or Krajcinovic and Lemaitre [KRA 87] and the literature cited therein. Following the attempts of Betten [BET 82] and Murakami [MUR 88], the well–known concept of deformed and reference, or rather undeformed, macroscopic configurations of a material body within the geometrically nonlinear continuum theory is supplemented by the concept of fictitious undamaged microscopic configuration. Nevertheless, in strong contrast to the classical approaches mentioned above, the present damage theory, fully outlined in Steinmann and Carol [STE 98] and further exploited in Menzel and Steinmann [MEN 00], is based on the notion of a second order damage metric tensor and its effects on the stored strain energy. Thereby, as the fundamental assumption, the storage of strain energy due to either nominal or effective strains is measured by either the damage or the energy metric based on the hypothesis of strain energy equivalence between microscopic and macroscopic configurations, see e.g. Sidoroff [SID 81]. The framework of standard dissipative materials, as proposed by Halphen and Nguyen [HAL 75] is strictly applied. Another approach to formulate anisotropic damage based on the introduction of an internal second order damage tensor similar to structural tensors has been given in Menzel and Steinmann [MEN 99].

2. Anisotropic hyper–elasticity based on a fictitious configuration

The reference and spatial configuration of the body of interest are denoted by $\mathcal{B}_0 \subset \mathbb{E}^3$ and $\mathcal{B}_t \subset \mathbb{E}^3$. Let $\boldsymbol{\varphi}(\boldsymbol{X}, t) : \mathcal{B}_0 \times \mathbb{R}_+ \to \mathcal{B}_t$ represent the non–linear map of material points $\boldsymbol{X} \in \mathcal{B}_0$ onto spatial points $\boldsymbol{x} = \boldsymbol{\varphi}(\boldsymbol{X}, t) \in \mathcal{B}_t$. In terms of convected coordinates $\theta^i(\boldsymbol{x})$ and $\Theta^i(\boldsymbol{X})$ the natural and dual base vectors are given by the derivatives $\boldsymbol{g}_i = \partial_{\theta^i}\boldsymbol{x} \in T\mathcal{B}_t$, $\boldsymbol{g}^i = \partial_{\boldsymbol{x}}\theta^i \in T^*\mathcal{B}_t$, $\boldsymbol{G}_i = \partial_{\Theta^i}\boldsymbol{X} \in T\mathcal{B}_0$ and $\boldsymbol{G}^i = \partial_{\boldsymbol{X}}\Theta^i \in T^*\mathcal{B}_0$. Now, the spatial and material metric tensors follow straightforward – $\boldsymbol{g}^\flat = g_{ij}\,\boldsymbol{g}^i \otimes \boldsymbol{g}^j$, $\boldsymbol{g}^\sharp = g^{ij}\,\boldsymbol{g}_i \otimes \boldsymbol{g}_j$, $\boldsymbol{G}^\flat = G_{ij}\,\boldsymbol{G}^i \otimes \boldsymbol{G}^j$, $\boldsymbol{G}^\sharp = G^{ij}\,\boldsymbol{G}_i \otimes \boldsymbol{G}_j$ – and in addition we introduce the mixed–variant identity–tensors $\boldsymbol{g}^\natural = \boldsymbol{g}_i \otimes \boldsymbol{g}^i$ and $\boldsymbol{G}^\natural = \boldsymbol{G}_i \otimes \boldsymbol{G}^i$. On this basis, the linear tangent map of the direct motion reads $\boldsymbol{F}^\natural = \partial_{\boldsymbol{X}}\boldsymbol{\varphi} = \partial_{\theta^i}\boldsymbol{\varphi} \otimes \partial_{\boldsymbol{X}}\theta^i = \boldsymbol{g}_i \otimes \boldsymbol{G}^i \in GL_+$ and, for notational simplicity, the gradient of the inverse motion $\Phi(x,t) = \varphi^{-1} : \mathcal{B}_t \times \mathbb{R}_+ \to \mathcal{B}_0$ reads $f^\natural = \partial_x \Phi = \partial_{\Theta^i}\Phi \otimes \partial_x \Theta^i = G_i \otimes g^i \in GL_+$. Several kinematic tensors can be introduced, e.g. the Finger tensors $b^\sharp = F^\natural \cdot G^\sharp \cdot [F^\natural]^t = G^{ij}\, g_i \otimes g_j$ or the right Cauchy–Green tensor $C^\flat = [F^\natural]^t \cdot g^\flat \cdot F^\natural = g^{ij}\, G^i \otimes G^j$ which enters the definition of the Green–Lagrange strain tensor $E^\flat = [C^\flat - G^\flat]/2$. A graphical representation is given in Figure 1 and in view of a detailed outline on non–linear kinematics we refer to the work of Marsden and Hughes [MAR 94].

2.1. The fictitious configuration

Now, in addition to the physical and material space we introduce a fictitious isotropic configuration with natural tangent space $T\bar{\mathcal{B}}_0$ and corresponding dual space $T^*\bar{\mathcal{B}}_0$. In analogy to the intermediate configuration within the multiplicative decomposition of elasto–plasticity, the fictitious configuration is generally incompatible. Mathematically speaking, we have a non–vanishing Riemann–Christoffel tensor which means that the conditions of compatibility are not fulfilled and the corresponding direct fictitious linear tangent map – denoted by $\bar{F}^\natural$ – takes the interpretation as a non–holonomic Pfaffian, see e.g. Haupt [HAU 00]. Nevertheless, within the proposed multiplicative composition $\bar{F}^\natural$ allows the interpretation as pre–stretch and defines the fictitious base vectors $\bar{G}_i \in T\bar{\mathcal{B}}_0$ and $\bar{G}^i \in T^*\bar{\mathcal{B}}_0$ which are obviously not derivable from position vectors. Next, the fictitious metric and identity–tensors follow as

$$\bar{G}^\flat = \bar{G}_{ij}\, \bar{G}^i \otimes \bar{G}^j\ ,\ \bar{G}^\sharp = \bar{G}^{ij}\, \bar{G}_i \otimes \bar{G}_j \ \text{ and }\ \bar{G}^\natural = \bar{G}_i \otimes \bar{G}^i\,. \tag{1}$$

The linear tangent maps due to the direct and inverse fictitious motion read

$$\bar{F}^\natural = G_i \otimes \bar{G}^i \ \text{ and }\ \bar{f}^\natural = \bar{G}_i \otimes G^i\,, \tag{2}$$

see Figure 1 for a graphical representation. Without loss of generality usual push–forward and pull–back operations in terms of the fictitious linear tangent map hold, e.g. $\bar{E}^\flat = [\bar{F}^\natural]^t \cdot E^\flat \cdot \bar{F}^\natural = [g_{ij} - G_{ij}]/2\, \bar{G}^i \otimes \bar{G}^j$.

2.2. Energy metric tensors

In the sequel we incorporate a contra–variant energy metric tensor which reads within the fictitious and undeformed setting as follows

$$\bar{A}^\sharp = \bar{A}^{ij}\, \bar{G}_i \otimes \bar{G}_j \ \text{ and }\ A^\sharp = A^{ij}\, G_i \otimes G_j \ \text{ with }\ \bar{G}^{ij} \doteq \bar{A}^{ij} = A^{ij}\,, \tag{3}$$

whereby the push–forward operation

$$A^\sharp = \bar{F}^\natural \cdot \bar{A}^\sharp \cdot [\bar{F}^\natural]^t \tag{4}$$

is implied. As a key idea, the fictitious energy metric tensor is chosen equal to the fictitious contra–variant metric tensor and replaces this metric within the construction

$$
\begin{tikzcd}
\mathcal{B}_0 \arrow[r, bend left, "\varphi(\boldsymbol{X},t)"] & \mathcal{B}_t \arrow[l, bend left, "\phi(\boldsymbol{x},t)"] \\
T\mathcal{B}_0 \arrow[r, shift left, "\boldsymbol{F}^\natural"] \arrow[d, shift left, "\bar{\boldsymbol{f}}^\natural"] & T\mathcal{B}_t \arrow[l, shift left, "\boldsymbol{f}^\natural"] \arrow[dl, shift right, "\bar{\boldsymbol{f}}^\natural \cdot \boldsymbol{f}^\natural"'] \\
T\bar{\mathcal{B}}_0 \arrow[u, shift left, "\bar{\boldsymbol{F}}^\natural"] \arrow[ur, shift right, "\boldsymbol{F}^\natural \cdot \bar{\boldsymbol{F}}^\natural"'] &
\end{tikzcd}
$$

Figure 1. *Non–linear point map φ and linear tangent maps $\bar{\boldsymbol{F}}^\natural$ and $\boldsymbol{F}^\natural$*

of the free Helmholtz energy function ψ_0. Consequently, due to the principle of strain energy equivalence the relation

$$\bar{\psi}_0(\bar{\boldsymbol{E}}^\flat, \bar{\boldsymbol{A}}^\sharp) = \psi_0(\boldsymbol{E}^\flat, \boldsymbol{A}^\sharp; \boldsymbol{X}) \tag{5}$$

holds, which means that the free Helmholtz energy remains invariant under the action of $\bar{\boldsymbol{F}}^\natural$.

Remark 2.1 *Note that eq.(5) includes all assumptions of the proposed framework. In particular isotropy is included if the energy metric tensor $\boldsymbol{A}^\sharp$ is spherical whereas otherwise anisotropy is considered. Since the relation $\bar{\boldsymbol{A}}^\sharp \doteq \bar{\boldsymbol{G}}^\sharp$ is incorporated, the fictitious configuration is isotropic and thus standard isotropic constitutive equation can be applied to model anisotropic material behaviour.*

Remark 2.2 *For conceptual simplicity we focus here on the composition $\boldsymbol{F}^\natural \cdot \bar{\boldsymbol{F}}^\natural$ and do not consider the spatial fictitious tangent space $T\bar{\mathcal{B}}_t$.*

2.3. Hyper–elasticity

Since the fictitious configuration is isotropic three (basic) invariants in terms of $\bar{\boldsymbol{E}}^\flat$ and $\bar{\boldsymbol{A}}^\sharp$ enter the formulation. Application of the standard pull–back operations $\bar{\boldsymbol{E}}^\flat = [\bar{\boldsymbol{F}}^\natural]^{\mathrm{t}} \cdot \boldsymbol{E}^\flat \cdot \bar{\boldsymbol{F}}^\natural$ and $\bar{\boldsymbol{A}}^\sharp = \bar{\boldsymbol{f}}^\natural \cdot \boldsymbol{A}^\sharp \cdot [\bar{\boldsymbol{f}}^\natural]^{\mathrm{t}}$ renders two corresponding sets of invariants

$${}^{\bar{E}^\flat \bar{A}^\sharp} I_n = \bar{\boldsymbol{G}}^\natural : [\bar{\boldsymbol{E}}^\flat \cdot \bar{\boldsymbol{A}}^\sharp]^n \quad \text{and} \quad {}^{E^\flat A^\sharp} I_n = \boldsymbol{G}^\natural : [\boldsymbol{E}^\flat \cdot \boldsymbol{A}^\sharp]^n \,, \tag{6}$$

with $n = 1, 2, 3$. Thus the usual hyper–elastic framework yields e.g the second Piola–Kirchhoff stress tensor

$$\boldsymbol{S}^\sharp = \partial_{\boldsymbol{E}^\flat} \psi_0 = \sum_{n=1}^{3} n \, \partial_{{}^{E^\flat A^\sharp} I_n} \psi_0 \; \boldsymbol{A}^\sharp \cdot [\boldsymbol{E}^\flat \cdot \boldsymbol{A}^\sharp]^{[n-1]} \tag{7}$$

and the Hessian ${}^{E^\flat E^\flat}\mathcal{L}^\sharp = \partial^2_{E^\flat \otimes E^\flat} \psi_0$ takes a similar format compared to standard isotropy.

2.4. Representation of the energy metric tensor

In order to demonstrate the nature of the energy metric tensor we choose the following ansatz for the fictitious contra–variant vectors $\bar{G}^i$ with respect to the anisotropic reference configuration $\mathcal{B}_0$ (with ${}^A\boldsymbol{N}^\flat_\zeta, {}^A\boldsymbol{N}^\sharp_\zeta \in S^2$)

$$\bar{G}^i = [\bar{F}^\natural]^{\mathrm{t}} \cdot G^i \doteq \alpha_0\, G^i + \sum\nolimits_{\zeta=1}^{2} \alpha_\zeta \; {}^A N^i_\zeta \; {}^A\boldsymbol{N}^\flat_\zeta \,. \tag{8}$$

With this representation in hand the two–field tensor $\bar{\boldsymbol{F}}^\natural = \boldsymbol{G}_i \otimes \bar{\boldsymbol{G}}^i$ reads

$$\bar{\boldsymbol{F}}^\natural \doteq \alpha_0\, \boldsymbol{G}^\natural + \sum\nolimits_{\zeta=1}^{2} \alpha_\zeta\, \boldsymbol{A}^\natural_\zeta \;\text{ with }\; \boldsymbol{A}^\natural_\zeta = {}^A\boldsymbol{N}^\sharp_\zeta \otimes {}^A\boldsymbol{N}^\flat_\zeta \,. \tag{9}$$

Now, straightforward computations due to eq.(4) with $\bar{\boldsymbol{A}}^\sharp \doteq \bar{\boldsymbol{G}}^\sharp$ render the symmetric energy metric tensor

$$\boldsymbol{A}^\sharp = \beta_0\, \boldsymbol{G}^\sharp + \beta_1\, \boldsymbol{A}^\sharp_1 + \beta_2\, \boldsymbol{A}^\sharp_2 + 2\,\beta_3\, [\boldsymbol{A}^\sharp_1 \cdot \boldsymbol{G}^\flat \cdot \boldsymbol{A}^\sharp_2]^{\mathrm{sym}} \,, \tag{10}$$

whereby the abbreviated notations $\beta_0 = \alpha_0^2$, $\beta_1 = 2\,\alpha_0\,\alpha_1 + \alpha_1^2$, $\beta_2 = 2\,\alpha_0\,\alpha_2 + \alpha_2^2$, $\beta_3 = \alpha_1\,\alpha_2$ have been applied.

Remark 2.3 *The rank one tensors $\boldsymbol{A}^\sharp_{1,2}$ allow similar interpretation as structural tensors. Indeed, the incorporation of eq.(10) into eq.(6) yields a set of invariants which can be expressed as a function of the set of invariants for general orthotropy as given e.g. by Spencer [SPE 84].*

Remark 2.4 *Within geometrically linear orthotropic hyper–elasticity based on structural tensors up to nine independent material parameters are included, see e.g. Spencer [SPE 84]. Contrary, the formulation based on the fictitious configuration incorporates four independent parameters (thereby the two Lamé constants are taken into account, and thus the additional isotropic parameter α_0 is not independent.) This underlines that we deal with a reduced formulation. For the sake of clarity, we consider the constant tangent operator of a material of linear St.–Venant Kirchhoff type ${}^{E^\flat E^\flat}\mathcal{L}^\sharp = \partial^2_{E^\flat \otimes E^\flat}\psi_0 \doteq \lambda\, \boldsymbol{A}^\sharp \otimes \boldsymbol{A}^\sharp + \mu\, [\boldsymbol{A}^\sharp \overline{\otimes}\, \boldsymbol{A}^\sharp + \boldsymbol{A}^\sharp \underline{\otimes}\, \boldsymbol{A}^\sharp]$. Now, referring to a Cartesian frame $\boldsymbol{e}_i$, we choose without loss of generality $\boldsymbol{A} \doteq \beta_0\, \boldsymbol{I} + \beta_1\, \boldsymbol{e}_1 \otimes \boldsymbol{e}_1 + \beta_2\, \boldsymbol{e}_2 \otimes \boldsymbol{e}_2$. Then, the relevant coefficients of the Hessian read*

$$\begin{array}{lll}
\mathcal{L}_{1111} = [\lambda + 2\mu][\eta_0 + \eta_1]^2 & \mathcal{L}_{1122} = \lambda[\eta_0 + \eta_1] & \mathcal{L}_{1133} = \lambda\eta_0[\eta_0 + \eta_1] \\
 & \qquad +2\mu[\eta_0 + \eta_2] & \\
\mathcal{L}_{2222} = [\lambda + 2\mu][\eta_0 + \eta_2]^2 & \mathcal{L}_{2233} = \lambda\eta_0[\eta_0 + \eta_2] & \mathcal{L}_{3333} = [\lambda + 2\mu]\eta_0^2 \\
\mathcal{L}_{1212} = \mu[\eta_0 + \eta_1][\eta_0 + \eta_2] & \mathcal{L}_{2323} = \mu\eta_0[\eta_0 + \eta_2] & \mathcal{L}_{1313} = \mu\eta_0[\eta_0 + \eta_1]
\end{array} \tag{11}$$

Obviously, we deal with a sub–class of rhombic symmetry.

2.5. Numerical examples

For the following numerical examples a non–linear material of Kauderer–type is applied, see Kauderer [KAU 49]. Within the general representation

$$\psi_0 = \psi_0(\boldsymbol{E}^\flat, \boldsymbol{A}^\sharp; \boldsymbol{X}) = \sum\nolimits_{p,q,r=0}^{\infty} c_{pqr} \; {}^{E^\flat A^\sharp}I_1^p \; {}^{E^\flat A^\sharp}I_2^q \; {}^{E^\flat A^\sharp}I_3^r \,, \tag{12}$$

compare Ogden [OGD 97], the coefficients of the implemented constitutive equation read:

$$\begin{array}{lll} c_{010} = G & c_{020} = \frac{2}{3}\, G\, \kappa_2^{\text{dev}} & c_{300} = \frac{1}{9}\, K\, \kappa_1^{\text{vol}} \\ c_{210} = -\frac{4}{9}\, G\, \kappa_2^{\text{dev}} & c_{600} = -\frac{16}{729}\, G\, \kappa_4^{\text{dev}} & c_{410} = \frac{16}{81}\, G\, \kappa_4^{\text{dev}} \\ c_{200} = \frac{1}{2}\, K - \frac{1}{3}\, G & c_{030} = -\, c_{220} = \frac{16}{27}\, G\, \kappa_4^{\text{dev}} & c_{400} = \frac{2}{27}\, G\, \kappa_2^{\text{dev}} + \frac{1}{12}\, K\, \kappa_2^{\text{vol}} \end{array} \tag{13}$$

The subsequent material parameters are chosen: $K = 8.333 \times 10^4$, $G = 3.8461 \times 10^4$, $\kappa_1^{\text{vol}} = \kappa_2^{\text{dev}} = 0.5$ and $\kappa_2^{\text{vol}} = \kappa_4^{\text{dev}} = 0.25$. In view of the energy metric tensor the following spherical coordinates define the orthogonal unit–vectors ${}^A\boldsymbol{N}_{1,2}$: $\vartheta_1^1 = 5/6\,\pi$, $\vartheta_1^2 = 1/6\,\pi$, $\vartheta_2^1 = 1/3\,\pi$ and $\vartheta_2^2 = 1/2\,\pi$, see the Appendix, and the additional scalars to compute $\bar{\boldsymbol{F}}^\natural$ read $\alpha_0 = 1.0$, $\alpha_1 = 0.25$ and $\alpha_2 = 0.5$.

2.5.1. Simple shear

For the homogeneous simple shear deformation ($\boldsymbol{F} = \boldsymbol{I} + \gamma\, \boldsymbol{e}_1 \otimes \boldsymbol{e}_2$ with $\boldsymbol{I} = \delta_{ij}\, \boldsymbol{e}_i \otimes \boldsymbol{e}_j$) Figures 2 and 3 highlight the anisotropic behaviour of the applied material, compare Appendix. The anisotropy measure δ shows a strong dependence on the shear number γ. Typically, the stereographic projection with respect to the stress and strain tensors underline their non–coaxiality. Finally, the plots of the determinant of the acoustic tensor show a different shape for the anisotropic and isotropic ($\alpha_1 = \alpha_2 = 0$) setting. They are given at $\gamma = 0.25$ in normalised form with respect to the linear isotropic case with $\det(\boldsymbol{q})^{\text{lin,iso}} = G^2\,[3/4\,G + K]$.

2.5.2. Cook's problem

A three–dimensional version of Cook's problem has been discretised with $16 \times 16 \times 4$ enhanced eight node bricks (Q1E9) as advocated by Simo and Armero [SIM 92]. Figure 4 shows the reference geometry ($L = 48$, $H_1 = 44$, $H_2 = 16$, $T = 4$), boundary conditions and a deformed mesh at $||\boldsymbol{F}|| = 1.28 \times 10^5$ which is the amount of the conservative resultant force of a continuous shear stress in $\mathcal{B}_0$. Furthermore, Figure 5 highlights the displacement of the mid point node at the top corner for the anisotropic meterial and in addition for an isotropic setting with ${}^{\text{iso}}\boldsymbol{A}^\sharp = [\beta_0^2 + [\beta_0 + \beta_1]^2 + [\beta_0 + \beta_2]^2]^{1/2}\, \boldsymbol{G}^\sharp$. Obviously the anisotropic case results in a non–vanishing component u_3 which indicates the "out–off–plane" deformation.

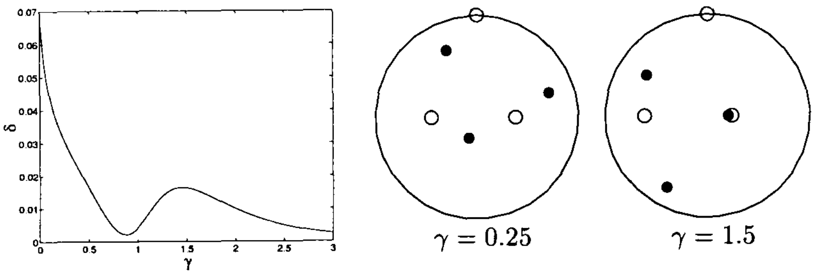

Figure 2. *Anisotropy measure δ and stereo–graphic projection due to the principal directions of strain $\boldsymbol{E}$: ∘ and stress $\boldsymbol{S}$: • with respect to a Cartesian frame*

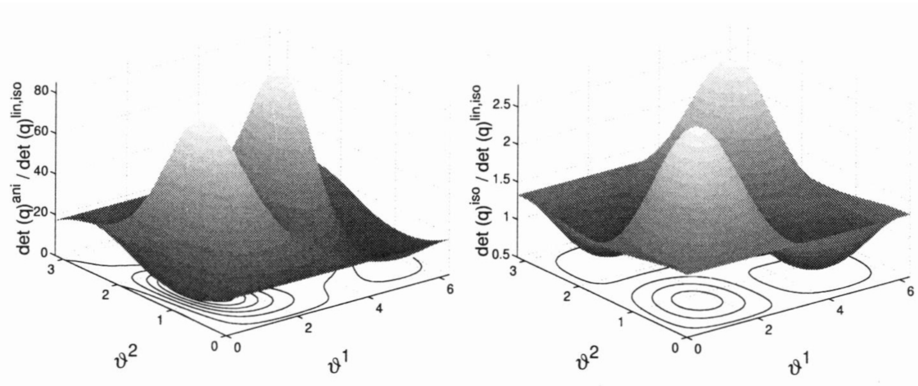

Figure 3. *Determinant of the acoustic tensor for $\gamma = 0.25$ within the anisotropic and the isotropic setting*

For more detailed background information on non–linear finite elements we refer e.g. to Oden [ODE 72]. Note that the proposed framework results in an efficient numerical setting. Practically, we end up with similar costs compared to isotropic hyper–elasticity, since the metric tensor $\boldsymbol{G}^\sharp$ of the standard formulation is replaced by $\boldsymbol{A}^\sharp$. Contrary the classical approach based on the incorporation of structural tensor yields numerous additional terms in the computation of the stress tensor and especially of the tangent operator which ends up with tremendous numerical costs.

3. Anisotropic damage based on a fictitious configuration

Here, as the key idea, the energy metric tensor is introduced as an internal variable and denoted as damage metric tensor in the sequel. Then the fictitious linear tangent map $\bar{\boldsymbol{F}}^\natural$ is no longer constant and allows the interpretation as damage deformation gradient. The fictitious configuration remains isotropic and un–damaged but the standard reference configuration $\mathcal{B}_0$ as well as the spatial one $\mathcal{B}_t$ can be damaged and anisotropic.

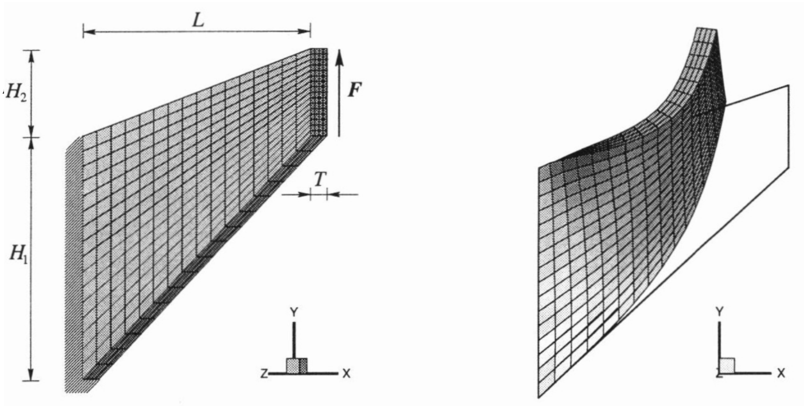

Figure 4. *Three–dimensional Cook's problem and deformed mesh at* $\|\boldsymbol{F}\| = 1.28 \times 10^5$

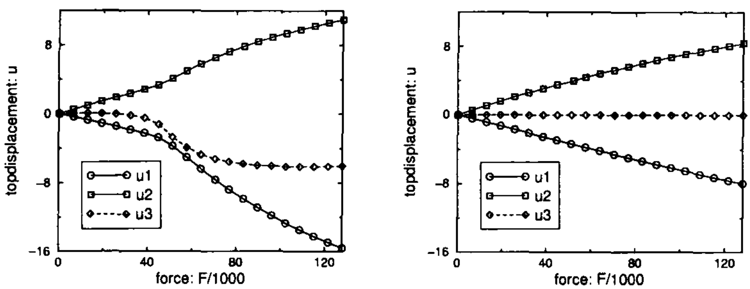

Figure 5. *Load–displacement curve of the mid point node at the top corner for the anisotropic and isotropic setting*

3.1. Standard dissipative materials

We adopt an additive decomposition of the free Helmholtz energy

$$\psi_0 = \psi_0^{\text{dam}}(\boldsymbol{E}^\flat, \boldsymbol{A}^\sharp; \boldsymbol{X}) + \psi_0^{\text{har}}(\kappa) \tag{14}$$

incorporating a scalar–valued hardening variable κ. Based on the theory of standard dissipative materials, see Halphen and Nguyen [HAL 75], the local form of the Clausius–Duhem inequality for the isothermal case with respect to $\mathcal{B}_0$ reads

$$\mathcal{D} = [\boldsymbol{S}^\sharp - \partial_{\boldsymbol{E}^\flat}\psi_0] : \mathrm{D}_t\boldsymbol{E}^\flat - \partial_{\boldsymbol{A}^\sharp}\psi_0 : \mathrm{D}_t\boldsymbol{A}^\sharp - \partial_\kappa\psi_0\, \mathrm{D}_t\kappa \geq 0\,. \tag{15}$$

Within the standard argumentation of rational thermodynamics the nominal stress, the damage stress and the hardening stress are obtained by

$$\boldsymbol{S}^\sharp = \partial_{\boldsymbol{E}^\flat}\psi_0 \quad \boldsymbol{\Delta}^\flat = -\,\partial_{\boldsymbol{A}^\sharp}\psi_0 \ \text{ and } \ H = \partial_\kappa\psi_0\,. \tag{16}$$

Next, an admissible elastic cone is introduced

$$\mathbb{A} = \left\{ (\boldsymbol{\Delta}^\flat, \boldsymbol{A}^\sharp, Y) \middle| \Phi = \Phi(\boldsymbol{\Delta}^\flat, \boldsymbol{A}^\sharp, Y) = \varphi(\boldsymbol{\Delta}^\flat, \boldsymbol{A}^\sharp) - Y \leq 0 \right\}, \tag{17}$$

whereby Φ is a convex function and $Y = Y_0 + H(\kappa)$. Moreover, associated evolution equations $\mathrm{D}_t \boldsymbol{A}^\sharp = \lambda\, \partial_{\boldsymbol{\Delta}^\flat} \Phi$, $\mathrm{D}_t \kappa = -\lambda\, \partial_H \Phi = \lambda$ are applied. The underlying constrained optimisation problem yields the Kuhn–Tucker conditions and the Lagrange multiplier λ can be computed via the consistency condition. Nevertheless, for the sake of demonstration, in the sequel the hardening contributions are assumed to be constant.

Remark 3.1 *Standard pull–back operations yield e.g.* $\bar{\boldsymbol{S}}^\sharp = \bar{\boldsymbol{f}}^\natural \cdot \boldsymbol{S}^\sharp \cdot [\bar{\boldsymbol{f}}^\natural]^{\mathrm{t}}$ *and* $\bar{\boldsymbol{\Delta}}^\flat = [\bar{\boldsymbol{F}}^\natural]^{\mathrm{t}} \cdot \boldsymbol{\Delta}^\flat \cdot \bar{\boldsymbol{F}}^\natural$ *which allow the interpretation as effective stress measures.*

3.2. Construction of the damage function

The specific form of the damage function significantly affects the evolution of anisotropic damage. Therefore, we will especially focus on the evolution of the eigendirections of the damage metric tensor.

The most general form is of course based on the set of ten invariants in terms of the damage stress $\boldsymbol{\Delta}^\flat$ and the damage metric $\boldsymbol{A}^\sharp$ itself

$$\varphi = \varphi({}^{\boldsymbol{\Delta}^\flat \boldsymbol{A}^\sharp} I_{1,\ldots,10}) \,. \tag{18}$$

Nevertheless, two selected representations seem to be natural and will be highlighted in the sequel, compare Schreyer [SCH 95].

The direct formulation introduces the damage rate negative proportional to a symmetric, positive semi–definite second order tensor ${}^2\boldsymbol{\Xi}^\sharp(\boldsymbol{A}^\sharp)$. Obviously, the simplest choice ${}^2\boldsymbol{\Xi}^\sharp \doteq \boldsymbol{A}^\sharp$ results in

$$\varphi_1 = -\boldsymbol{A}^\sharp : \boldsymbol{\Delta}^\flat \;\longrightarrow\; \mathrm{D}_t \boldsymbol{A}^\sharp = -\lambda\, \boldsymbol{A}^\sharp \tag{19}$$

and the dissipation inequality reads $\mathcal{D} = \lambda Y \geq 0$. Indeed, the damage rate and the damage metric itself are coaxial but since the damage metric could be non–spherical we denote this type of damage as *quasi isotropic*.

The formulation based on conjugate variables constructs the damage rate as a linear map of the damage stress via a symmetric, positive semi–definite fourth order tensor ${}^4\boldsymbol{\Xi}^\sharp(\boldsymbol{A}^\sharp)$. Again, a simple choice ${}^4\boldsymbol{\Xi}^\sharp \doteq \boldsymbol{A}^\sharp \,\overline{\otimes}\, \boldsymbol{A}^\sharp$ ends up with the quadratic form

$$\varphi_2 = 1/2\, \boldsymbol{\Delta}^\flat : [\boldsymbol{A}^\sharp \,\overline{\otimes}\, \boldsymbol{A}^\sharp] : \boldsymbol{\Delta}^\flat \;\longrightarrow\; \mathrm{D}_t \boldsymbol{A}^\sharp = \lambda\, \boldsymbol{A}^\sharp \cdot \boldsymbol{\Delta}^\flat \cdot \boldsymbol{A}^\sharp \tag{20}$$

and the reduced local form of the Clausius–Duhem inequality reads $\mathcal{D} = 2\,\lambda\, Y \geq 0$. Obviously, the damage rate and the damage metric are no longer coaxial which motivates the terminology *anisotropic damage*.

Remark 3.2 *Eqs.(19,20) can alternatively be motivated via the following quadratic form*

$$^{G^\sharp}\varphi = \boldsymbol{\Delta}^\flat : \left[\eta_1\, \boldsymbol{G}^\sharp \otimes \boldsymbol{G}^\sharp + \eta_2 \left[\boldsymbol{G}^\sharp \,\overline{\otimes}\, \boldsymbol{G}^\sharp + \boldsymbol{G}^\sharp \,\underline{\otimes}\, \boldsymbol{G}^\sharp\right]\right] : \boldsymbol{\Delta}^\flat\,, \tag{21}$$

whereby for the fourth order tensor $^4\Xi$ *the structure of the tangent operator of linear elasticity has been adopted. Now, due to the central idea of the proposed framework, the contra–variant metric tensor is replace by the damage metric*

$$^{A^\sharp}\varphi = \boldsymbol{\Delta}^\flat : \left[\eta_1\, \boldsymbol{A}^\sharp \otimes \boldsymbol{A}^\sharp + \eta_2 \left[\boldsymbol{A}^\sharp \,\overline{\otimes}\, \boldsymbol{A}^\sharp + \boldsymbol{A}^\sharp \,\underline{\otimes}\, \boldsymbol{A}^\sharp\right]\right] : \boldsymbol{\Delta}^\flat\,. \tag{22}$$

Then the first term, incorporating the scalar η_1*, represents the quasi isotropic damage function* φ_1 *of eq.(19) and the second term, incorporating the scalar* η_2*, represents the anisotropic damage function* φ_2 *of eq.(20).*

Remark 3.3 *In contrast to isotropy the incorporation of an in–elastic potential together with the application of associated evolution equations within an anisotropic setting is an assumption since the obtained rate equations represent reduced forms of the most general tensor functions in terms of all appropriate arguments, see e.g. Betten [BET 85].*

Remark 3.4 *The two introduced types of damage functions and the character of the initial damage metric tensor* $\boldsymbol{A}_0^\sharp$ *define a general classification of the coupling of hyper–elasticity and damage. In particular, the following four categories are obtained:*

(1) isotropic hyper–elasticity ($\boldsymbol{A}_0^\sharp = \beta_0\, \boldsymbol{G}^\sharp$*) & quasi isotropic damage (*φ_1*)*
(2) isotropic hyper–elasticity ($\boldsymbol{A}_0^\sharp = \beta_0\, \boldsymbol{G}^\sharp$*) & anisotropic damage (*φ_2*)*
(3) anisotropic hyper–elasticity ($\boldsymbol{A}_0^\sharp \neq \beta_0\, \boldsymbol{G}^\sharp$*) & quasi isotropic damage (*φ_1*)*
(4) anisotropic hyper–elasticity ($\boldsymbol{A}_0^\sharp \neq \beta_0\, \boldsymbol{G}^\sharp$*) & anisotropic damage (*φ_2*)*

Assuming a material of St. Venant–Kirchhoff type category (1) is directly related to the classical $[1 - d]$ *damage formulation via* $\boldsymbol{A}^\sharp = \beta_0\, \boldsymbol{G}^\sharp = [1 - d]^2\, \boldsymbol{G}^\sharp$*. In this case* β_0 *represents three equal eigenvalues, which degrade for increasing damage, e.g. characterised by d. Moreover, note that especially formulations within category (2) become anisotropic within the purely elastic domain for unloading after damage evolution has taken place.*

3.3. Numerical examples

In the sequel we apply a compressible Mooney–Rivlin material of the form

$$\begin{aligned} \psi_0 &= c_1\,[\,^{C^\flat G^\sharp}J_1 - 3] + c_2\,[\,^{C^\flat G^\sharp}J_2 - 3] \\ &+ \lambda^p \ln^2\left(^{C^\flat G^\sharp}J_3^{1/2}\right) - 2[c_1 + 2\,c_2]\,\ln\left(^{C^\flat G^\sharp}J_3^{1/2}\right), \end{aligned} \tag{23}$$

whereby the principal invariants $^{C^\flat G^\sharp}J_{1,2,3}$ are expressed in terms of the basic invariants ${}^{E^\flat A^\sharp}I_{1,2,3}$, to be specific

$$
\begin{aligned}
{}^{C^\flat G^\sharp}J_1 &= 3 + 2\ {}^{E^\flat A^\sharp}I_1 \\
{}^{C^\flat G^\sharp}J_2 &= 3 + 4\ {}^{E^\flat A^\sharp}I_1 - 2\ {}^{E^\flat A^\sharp}I_2 + 2\ {}^{E^\flat A^\sharp}I_1^2 \\
{}^{C^\flat G^\sharp}J_3 &= 1 + 2\ {}^{E^\flat A^\sharp}I_1 - 2\ {}^{E^\flat A^\sharp}I_2 + 8/3\ {}^{E^\flat A^\sharp}I_3 \\
&+ 2\ {}^{E^\flat A^\sharp}I_1^2 - 4\ {}^{E^\flat A^\sharp}I_1\ {}^{E^\flat A^\sharp}I_2 + 4/3\ {}^{E^\flat A^\sharp}I_1^3 \,.
\end{aligned} \tag{24}
$$

In order to define the initial damage metric tensor we chose the specific format $\boldsymbol{A}_0^\sharp = \gamma_0\, \boldsymbol{G}^\sharp + \sum_{\varsigma=1}^{2} \gamma_\varsigma\ {}^{A}\boldsymbol{N}_\varsigma^\sharp \otimes {}^{A}\boldsymbol{N}_\varsigma^\sharp$, compare Svendsen [SVE]. Moreover, the following material parameter have been taken into account $c_1 = 10$, $c_2 = 20$, $\lambda^p = 5$, $\gamma_0 = 1.0$, $\gamma_1 = 0.5$, $\gamma_2 = 0.25$, $Y = 10$ and the orthogonal unit–vectors ${}^{A}\boldsymbol{N}_{1,2}^\sharp$ are define by spherical coordinates $\vartheta_1^1 = 2/3\,\pi$, $\vartheta_1^1 = 1/3\,\pi$, $\vartheta_1^1 = 4/3\,\pi$, $\vartheta_1^1 = 1/6\,\pi$ (compare Appendix). For quasi isotropic damage (φ_1) an exponential integration scheme is available whereas for anisotropic damage evolution (φ_2) an implicit Euler backward scheme is applied. We do not focus on numerical aspects here since they are discussed in detail in Menzel and Steinmann [MEN 00]. Within the following finite element setting the tangent operator has been evaluated numerically as e.g. outlined in Miehe [MIE 96].

3.3.1 Simple shear

We consider again the homogeneous deformation of simple shear $(\boldsymbol{F} = \boldsymbol{I} + \gamma\, \boldsymbol{e}_1 \otimes \boldsymbol{e}_2)$ and take anisotropic damage (φ_2) into account. Figure 6 shows the different degradations of the eigenvalues of the damage metric tensor and highlights the non–coaxiality of stress and strain, compare Appendix. In addition the stereographic projection of the principal damage directions are given which evolve during the deformation process.

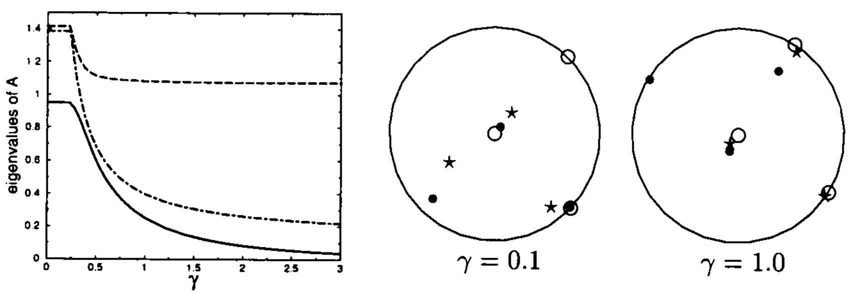

Figure 6. *Degradation of the eigenvalues ${}^{A}\lambda_{1,2,3}$ and stereo–graphic projection due to the principal directions of strain $\boldsymbol{E}$: ∘, stress $\boldsymbol{S}$: • and the damage metric $\boldsymbol{A}$: ⋆ with respect to a Cartesian frame*

3.3.2 Strip with a hole

To give a three–dimensional finite element example a strip with a hole is discretised by 64 × 2 enhanced eight node bricks (Q1E9) as advocated by Simo and Armero [SIM 92]. The geometry of the specimen is defined by a length of 12, a width of 4, a thickness of 0.5 and a radius of 1. One end is totally clamped while the other end is subject to displacement conditions in longitudinal direction. Figure 7 shows the deformed mesh and the anisotropy measure δ for a maximal longitudinal stretch of $\lambda = 1.5$ for the purely hyper–elastic solution ($Y \to \infty$). In addition the load–displacement curve of the mid node at the un–clamped end underlines the anisotropic behaviour since the displacement components u_1 and u_3 would be identical to zero within an isotropic setting. Now, incorporating damage evolution the degradation is concentrated (un–symmetrically) at the boundary of the hole. In this context Figure 8 highlights the smallest eigenvalue ${}^A\lambda_1$ of the damage metric tensor and the anisotropy measure δ within quasi isotropic damage (φ_1). Moreover, Figure 9 visualises the same contents for anisotropic damage (φ_2).

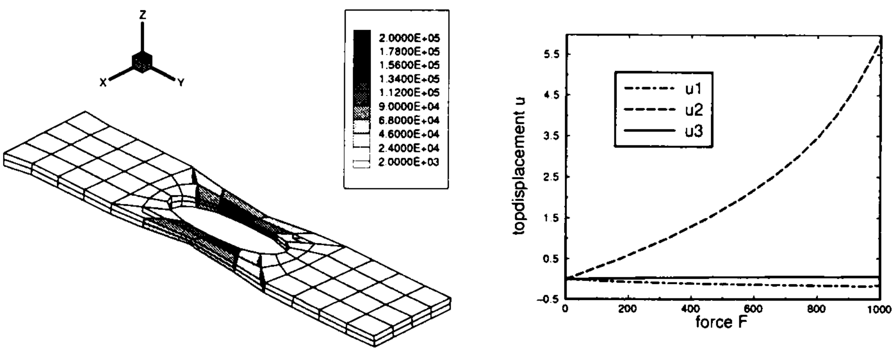

Figure 7. *Anisotropy measure δ and deformed mesh for a maximal longitudinal stretch $\lambda = 1.5$ and load–displacement curve of the un–clamped mid point node at the free end within pure hyper–elasticity ($Y \to \infty$)*

4. Outlook

The proposed thermodynamically consistent framework for anisotropic materials at large strains results in a manageable numerical setting. Nevertheless, concerning future work, localisation has somehow to be taken into account. Furthermore, the coupling to finite strain plasticity is an outstanding issue and finally the construction of specific damage functions for engineering material as well as the corresponding identification of material parameters are important areas constituting future research.

Appendix: Visualisation of Anisotropy

Especially for three–dimensional examples it is not a trivial task to visualise anisotropy. In the sequel three different propositions are made.

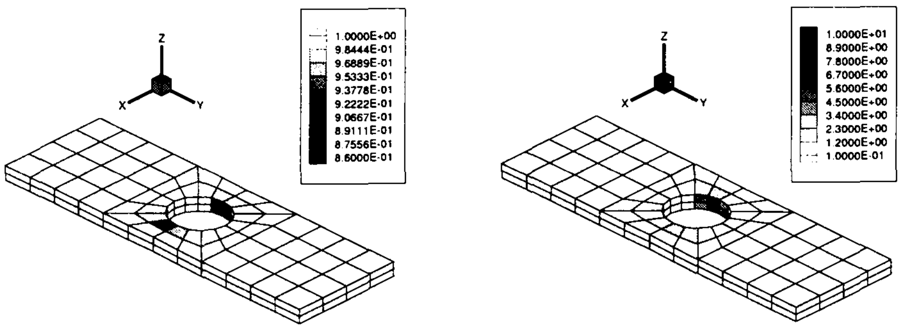

Figure 8. *Smallest eigenvalue* ${}^{A}\lambda_1$ *of the damage metric and anisotropy measure* δ *for quasi isotropic damage* (φ_1) *at* $\|\boldsymbol{F}\| = 114$

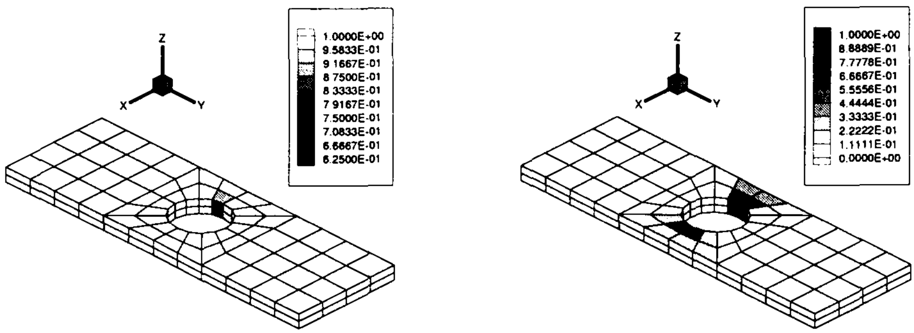

Figure 9. *Smallest eigenvalue* ${}^{A}\lambda_1$ *of the damage metric and anisotropy measure* δ *for anisotropic isotropic damage* (φ_2) *at* $\|\boldsymbol{F}\| = 65$.

In case that stress and strain tensors are not coaxial we deal with an anisotropic material. This motivates the introduction of the *anisotropy measure*

$$\delta = \|\boldsymbol{G}^\flat \cdot \boldsymbol{S}^\sharp \cdot \boldsymbol{E}^\flat - \boldsymbol{E}^\flat \cdot \boldsymbol{S}^\sharp \cdot \boldsymbol{G}^\flat\| \,/\, [\, \|\boldsymbol{S}^\sharp\| \, \|\boldsymbol{E}^\flat\| \,] \, . \tag{25}$$

Within the method of *stereographic projection* the eigenvectors of a symmetric second order tensor – which allow interpretation of being elements of the unit–sphere S^2 – are projected onto the equatorial plane by viewing from the south pole. Mathematically speaking, this method represents the homomorphism $SO(3) \to SU(2)$, see e.g. Altmann [ALT 86].

Determinant of the acoustic tensor: Incorporating the common wave equation ansatz into the incremental equation of motion for $\boldsymbol{F}^\natural \doteq$ const yields (see e.g. Antman [ANT 95])

$$\boldsymbol{q}^\natural = [[\boldsymbol{g}^\natural \otimes \boldsymbol{N}^\flat] : {}^{t}\boldsymbol{\mathcal{L}}^\natural \cdot \boldsymbol{N}^\flat + [\boldsymbol{N}^\flat \cdot \boldsymbol{S}^\sharp \cdot \boldsymbol{N}^\flat]\, \boldsymbol{g}^\natural] \tag{26}$$

with ${}^{t}\boldsymbol{\mathcal{L}}^\natural = \boldsymbol{F}^\natural \cdot {}^{E^\flat E^\flat}\boldsymbol{\mathcal{L}}^\sharp : [[[\boldsymbol{F}^\natural]^t \cdot \boldsymbol{g}^\flat] \,\overline{\otimes}\, [\boldsymbol{G}^\natural]^t]$ and $\boldsymbol{N}^\flat = [\boldsymbol{F}^\natural]^t \cdot \boldsymbol{n}^\flat$, whereby the spatial unit–vector $\boldsymbol{n}^b \in S^2$ can be defined by two spherical coordinates $\vartheta^{1,2}$. Referring to a Cartesian frame $\boldsymbol{e}_i$, one of three possible parametrisations to define $\boldsymbol{n} = n^i \boldsymbol{e}_i \in S^2$ reads

$$n^1 \doteq \sin(\vartheta^1)\,\sin(\vartheta^2)\,,\; n^2 \doteq \cos(\vartheta^2)\,,\; n^3 \doteq \cos(\vartheta^1)\,\sin(\vartheta^2)\,. \tag{27}$$

5. References

[ALT 86] ALTMANN S. L. *Rotation, Quaternions and Double Groups*. Oxford University Press, 1986.

[ANT 95] ANTMAN S. S. *Nonlinear Problems of Elasticity*. Number 107 in Applied Mathematical Sciences. Springer, 1995.

[BET 82] BETTEN J. « Net-stress analysis in creep mechanics ». *Ing. Arch.*, 52:405–419, 1982.

[BET 85] BETTEN J. « The classical plastic potential theory in comparison with the tensor function theory ». *Eng. Fract. Mech.*, 21(4):641–652, 1985.

[HAL 75] HALPHEN B. AND NGUYEN Q.S. « Sur les matériaux standards généralisés ». *J. Mécanique*, 14:39–62, 1975.

[HAU 00] HAUPT P. *Continuum Mechanics and Theory of Materials*. Advanced Texts in Physics. Springer, 2000.

[KAU 49] KAUDERER H. « Über ein nichtlineares Elastizitätsgesetz ». *Ingenieur–Archiv*, XVII:450–480, 1949.

[KRA 87] KRAJCINOVIC D. AND LEMAITRE J. *Continuum Damage Mechanics*. Number 295 in CISM Courses and Lectures. Springer, 1987.

[LEM 96] LEMAITRE J. *A Course on Damage Mechanics*. Springer, 2nd edition, 1996.

[MAR 94] MARSDEN J.E. AND HUGHES T.J.R. *Mathematical Foundations of Elasticity*. Dover, 1994.

[MEN 99] MENZEL A. AND STEINMANN P. « A theoretical and computational setting for geometrically nonlinear damage mechanics ». In WUNDERLICH W., Ed., *Proceedings of the European Conference on Computational Mechanics*, number 329. ECCM, Munich, 31.08.– 03.09. 1999.

[MEN 00] MENZEL A. AND STEINMANN P. « A theoretical and computational setting for anisotropic continuum damage mechanics at large strains ». *Int. J. Solids & Structures*, 2000. accepted for publication.

[MIE 96] MIEHE C. « Numerical computation of algorithmic (consistent) tangent moduli in large–strain computational inelasticity ». *Comp. Meth. Appl. Mech. Engrg.*, 134:223–240, 1996.

[MUR 88] MURAKAMI S. « Mechanical modeling of material damage ». *ASME J. Appl. Mech.*, 55, 1988.

[ODE 72] ODEN J.T. *Finite Elements of Nonlinear Continua*. Advanced Engineering Series. McGraw–Hill, 1972.

[OGD 97] OGDEN R.W. *Non–Linear Elastic Deformations*. Dover, 1997.

[SCH 95] SCHREYER H.L. « Continuum damage based on elastic projection tensors ». *Int. J. Damage Mechanics*, 4:171–195, 1995.

[SID 81] SIDOROFF F. « Description of anisotropic damage application to elasticity ». In HULT J. AND LEMAITRE J., Eds, *Physical Non–Linearities in Structural Analysis*. IUTAM Symposium Senlis/France, Springer, 27.–30.05. 1981.

[SIM 92] SIMO J.C. AND ARMERO F. « Geometrically non–linear enhanced strain mixed methods and the method of incompatible modes ». *Int. J. Num. Meth. Eng.*, 33:1413–1449, 1992.

[SPE 84] SPENCER A.J.M. « Constitutive theory of strongly anisotropic solids ». In SPENCER A.J.M., Ed., *Continuum Theory of the Mechanics of Fibre–Reinforced Composites*, number 282 in CISM Courses and Lectures. Springer, 1984.

[STE 98] STEINMANN P. AND CAROL I. « A framework for geometrically nonlinear continuum damage mechanics ». *Int. J. Engng. Sci.*, 36:1793–1814, 1998.

[SVE] SVENDSEN B. On the modeling of anisotropic elastic and inelastic material behaviour at large deformation. Preprint.